

Effect of Lower Convective Zone Thickness and Swirl Flow on the Performance of a Salinity Gradient Solar Pond

Karunamurthy Krishnasamy*, Manimaran Renganathan

School of Mechanical and Building Sciences, VIT University, Chennai 600127, India
karunamurthy.k@gmail.com

Solar ponds collect solar radiation and store it in the form of thermal energy over a period of time. The performance of a solar pond depends upon the performance of the heat exchange process. In this study, a laboratory model solar pond was fabricated and provided with an in-pond heat exchanger. To perform the computational study the lower convective zone (LCZ) of the solar pond alone was modelled using ANSYS Design Modeler. The analysis was carried out on the plain tube in-pond heat exchanger of the solar pond for different heights of LCZ for two different flow rates of heat transfer fluid. The performance parameters such as outlet water temperature, rate of heat transfer, effectiveness of heat exchanger, and pressure drop were analysed. The rate of heat transfer, pressure drop, Nusselt number and effectiveness of heat exchanger are evaluated by changing the velocity vectors of the fluid flow at the entrance of the in-pond heat exchanger. The rate of heat transfer is found to be higher for turbulent flow than laminar flow for different temperatures of LCZ.

1. Introduction

Salinity gradient solar ponds are pools of salt water having increasing density with depth in the pond; thereby preventing bulk motion of the fluid and arresting convection. In order to achieve the varying density within the pond, three different zones namely Lower convective zone (LCZ), Non-Convective Zone (NCZ) and Upper Convective Zone (UCZ) are maintained in a SGSP. The thermal energy collected is stored in the LCZ of the SGSP and this thermal energy is exchanged using heat exchangers. This heat exchanger can be internal or external to the SGSP. In this paper, an internal heat exchanger was considered for analysis. Solar ponds are used for various applications including process heating, power generation, refrigeration and air conditioning. Alcaraz et al., (2016) extracted heat from both the gradient and heat storage zones of a pilot SGSP using lateral and bottom heat exchangers. Behrooz et al., (2016) compared two-phase closed thermosyphons with the single-phase mode heat transfer using an enhanced design of a large scale SGSP power plant. Ding et al (2016) developed a transient model to predict the performance of thermoelectric generators coupled with solar ponds. It has strong influence in initial stage of pond to warm up. Ganesh and Arumugam (2016) studied the performance of a laboratory model shallow solar pond (SSP) with and without a single transparent glass cover for solar thermal energy conversion applications. They suggested SSP water heater for roof top solar energy collection. It was also found that SSP solar collection efficiency was 40 % which is comparable to flat plate collector systems. Assad et al., (2016) developed a model to determine the outlet temperature of a solar pond using MATLAB. Their results depicted that maximum loss of thermal energy was mainly due to evaporation from the surface of the pond. Mohammad (2015) investigated experimentally the absorption of heat of different solar pond shapes covered with plastic glazing. The study also focussed on the geometry of the SGSP, and the effect of weather condition on solar pond temperature. The results revealed that the phase change material (PCM) reduced the thermal efficiency of the solar pond, increased the thermal stability of the solar pond and solar pond with PCM leads to more salinity against heat extraction. In Tibet, to speed up the temperature rise of brine to produce lithium carbonate, large scale solar ponds were used. The effect of sunny area ratio on solar ponds with different geometries was studied by Ismail and Mehmet (2015). A comprehensive experimental work on the turbidity of the solar pond was carried out by Ayhan et al., (2014). The study evaluated the percentage transmission of turbid and clean salty water of the zones. The thermal performance of the SGSP was assessed by comparing the exergetic efficiencies of the solar pond. In the

recent literatures on heat exchanger Suraya Hanim Abu Bakar et al., (2017) carried out an industrial case study application in synthesizing a feasible heat exchanger network to minimize the total annual cost. The individual heat exchanger and overall heat exchanger network risks were analysed and different risk limits have been imposed while synthesizing the heat exchanger network by Andreja Nemet et al., (2017). Heat transfer and losses of exergy in a double pipe heat exchanger with semi elliptical corrugations were investigated by Pesteei et al., (2017) and found that higher heat transfer rate increased the exergy losses. Dipankar De et al., (2017) found significant increase in heat transfer coefficient per unit pressure drop in the case of heat exchanger with helical baffle compared to straight baffle plates. A method by Pullela et al., (2017) to estimate the critical period of maintenance of heat exchanger was suggested by considering time dependent fouling factors for parallel and counter flow heat exchangers.

From the literature, many studies are reported for the performance enhancement of solar ponds. It is well known that internal heat exchangers outweigh the externally placed heat exchangers in terms of performance. However, the study of flow in the internal heat exchanger is limited in literature. In this study, experiments and conjugate heat transfer analyses are carried out using computational fluid dynamic approach with respect to several cases considered for the internal heat exchanger. Heat exchangers are found to be located in the bottom of solar pond and the dimensions of the model are considered as per Huseyin et al., (2006). The non-dimensional numbers are compared between small and large ponds and found to be in conformity with literature. Outlet temperature of heat exchanger, heat transfer rate, pressure drop, Nusselt number and effectiveness are reported from this study.

2. Experimental Setup

A laboratory model solar pond was fabricated using 1.5 mm thick galvanised iron sheet with dimensions of 1.2 m(L)X1m(W)X0.6m(H). The SGSP was filled with saline water and three different zones were maintained with the following densities; LCZ of 1200 kg/m³, NCZ of 1100 kg/m³ and UCZ of 1000 kg/m³. The pond was covered with transparent plastic sheet and left for three days to allow any molecular diffusion. The inner surface of the SGSP was painted black, whereas the outer surface was insulated using glass wool and Styrofoam of thickness 10 mm each. Sampling vents were provided to measure the density of the zones during the study. Thermocouples of 'J' type (iron-constantan) and digital temperature indicator are used to determine the following average temperatures: ambient temperature (T_1), temperature of UCZ (T_2), temperature of NCZ (T_3), temperature of LCZ (T_4), water inlet temperature (T_5), water outlet temperature (T_6).

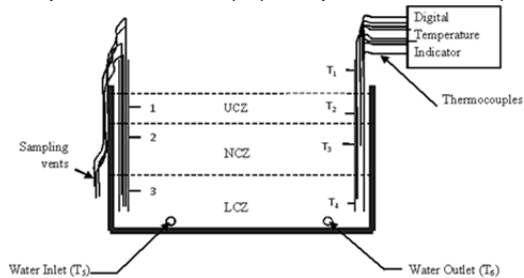


Figure 1: Schematic diagram of laboratory model SGSP

The zone temperatures are measured at two different locations on opposite sides of the SGSP and the average temperature is considered. The detailed schematic diagram of the SGSP is represented in Figure 1. The heat exchange process in the SGSP is achieved by providing a five pass heat exchanger of copper tube of 12 mm outer diameter and 10.5 mm inner diameter. The heat transfer fluid is water which flows at a rate of 0.0086 kg/s for laminar flow ($Re=1595$) and 0.0433 kg/s for turbulent flow ($Re=7979$). The temperatures are measured at regular intervals of 30 minutes from morning 08:00 am to 06:00 pm in the evening in the month of May 2016 at Chennai, India. In the experiments, the height (thickness) of LCZ of the SGSP was maintained as in Table 1.

Table 1: Different heights of zones of SGSP considered for CFD study

Case	Height of LCZ	Height of NCZ	Height of UCZ
Case H1	200 mm	200 mm	100 mm
Case H2	250 mm	150 mm	100 mm
Case H3	150 mm	250 mm	100 mm

3. Computational Model

The SGSP was modelled using ANSYS Design Modeler and analysed using ANSYS-FLUENT software. The LCZ of the SGSP with heat exchanger alone was modelled and boundary conditions were provided to perform the computational study. The modelled SGSP and the meshed model are represented in Figure 2 and Figure 3. The computational analysis was done by providing the temperature of the LCZ. The variation in the temperature of the LCZ in a day was obtained from the experimentation carried out and they also form the different cases of computational study for laminar and turbulent flows as shown in Table 2. The timings in a day during May 2016 at Chennai, India during which the above mentioned temperatures were observed are from 08:00 to 18:00 hours at every 30 minutes.

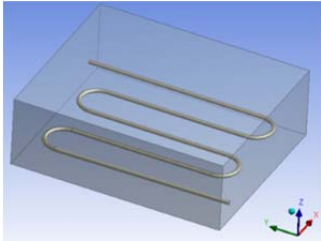


Figure 2: Lower convective zone model in SGSP

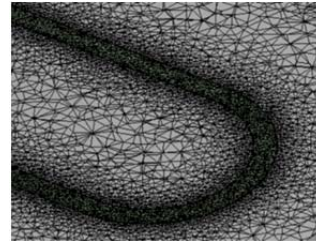


Figure 3: Mesh showing the LCZ region with heat exchanger pipe wall and internal fluid

Table 2: Different cases of computational study corresponding to temperatures of LCZ

Time	08:00	08:30	09:00	09:30	10:00	10:30	11:00	11:30	12:00	12:30	13:00
T_{LCZ} (K)	300	303	306	309	313	317	321	325	330	335	340

3.1 Computational Analysis and Sample Outputs

The study of the internal flow field in the heat exchanger tube of the salinity gradient solar pond is found to be very difficult to analyse by physical experiments. However limited experimental studies are conducted for the validation purpose of CFD simulations. The CFD model is replicated as per the experimental model discussed before. The steady state calculations are performed by conjugate heat transfer analysis using CFD. The side walls are adiabatic. The bottom wall temperatures as measured by experiments are fed as input to numerical study. Inlet mass flow rate of the heat exchanger is specified from experimental studies. No solar heat generation inside the LCZ is considered. The heat exchanger is placed at a height of 5 cm above the bottom of the pond. Reynolds stress turbulence model is used to consider the effects of buoyancy near the pipe wall. Steady-state SIMPLE solver and second order upwind schemes for the continuity, momentum and energy equations are employed to perform the computation.

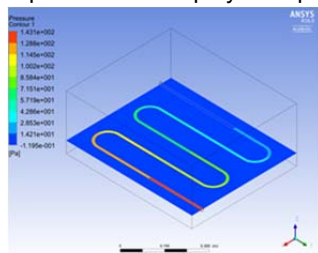


Figure 4a: Pressure distribution

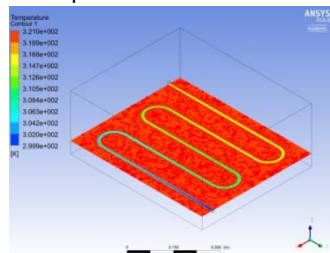


Figure 4b: Temperature profile

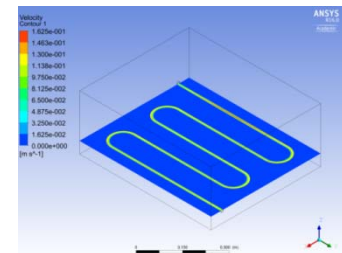


Figure 4c: Velocity Profile

To account for turbulent flow, standard k- ϵ model is employed with turbulent intensity of 5% at inlet. The boundary conditions for all the cases are maintained with 0.1m/s and 0.5m/s velocities at inlet to the tube for laminar and turbulent flows respectively. The exit boundary condition is imposed as pressure outlet (ambient pressure). The temperatures of the LCZ are given in Table 2. Numerical computations are performed to understand the nature of flow field and heat transfer. Table 3 shows the grid independency study results for different grid sizes. The mesh size is considered from 1 million to 5 million nodes. The temperature at the outlet of the heat exchanger tube does not vary significantly after a mesh size of 4 million nodes. Hence the same mesh size is used for further cases. It is also found later that this mesh size yields result closer to

experimental result. The comparison of results between CFD and experiments are found and the maximum error between the two is less than 1.14 %.

Table 3: Grid Dependency Test

Sl. No	Number of Cells	T6 (K)
1	5,00,000	326.7
2	12,50,000	325.3
3	25,00,000	320.8
4	37,50,000	317.6
5	50,00,000	314.7

Table 4: Various cases of swirl flow in CFD study

	Case	T ₅ (K)	T ₄ (K)	Tangential	Axial	Radial	T ₆ (K)
				U (%)	V	W (%)	
Laminar (Re=1595)	1	300	340	No Swirl (0.1 m/s)			314.5
	2	300	340	12.5	75%	12.5	315.9
	3	300	340	25	50%	25	317.7
	4	300	340	37.5	25%	37.5	319.3
Turbulent (Re=7979)	5	300	340	No Swirl (0.5 m/s)			308.5
	6	300	340	12.5	75%	12.5	309.2
	7	300	340	25	50%	25	309.8
	8	300	340	37.5	25%	37.5	310.5

The sample pressure, temperature and velocity profiles of the fluid flow through the heat exchanger of the SGSP corresponding to laminar flow for a LCZ height of 200mm and LCZ temperature of 340K are shown in Figure 4a, Figure 4b and Figure4c respectively. Experimental measurements of LCZ temperatures are plotted in Figure 5.

In order to increase the rate of heat exchange process, an attempt was made to create swirl in the flow field of the heat exchanger tube by varying the velocity vectors. Swirl is being created along the radial, axial and tangential directions of flow. The swirl is introduced at the inlet to increase the heat transfer. The swirl creates turbulence inside the flow passage and increases the residence time. This enhances the heat transfer between LCZ and heat exchanger. The flow components are divided as tangential, axial and radial components of velocity as mentioned in Table 4. For no swirl condition, only axial component is considered. It was observed that, swirl in the flow resulted in better mixing of the heat transfer fluid and leading to better rate of heat transfer. It was also inferred that swirl is more effective for laminar flow compared to turbulent flow. The different swirl cases of analysis are in Table 4.

4. Results and Discussion

The pressure drop for laminar and turbulent are indicated in Figure 5 and Figure 6. It is obvious that the pressure drop is higher for turbulent flow compared to laminar flow. The pressure drop equation for laminar flow is given with respect to friction factor ($\Delta p=fLv^2/2gD$). It is found that 22 % of the pressure drop occurs at the bend. According to pipe flow theory, the pressure drop magnitudes are found to be 145Pa and 1244Pa for laminar and turbulent flows respectively. The temperatures observed in LCZ during morning and evening varies because of storage of thermal energy upto peak sunshine time and release of thermal energy thereafter.

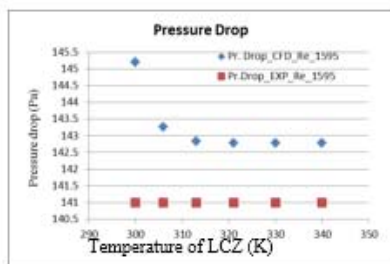


Figure 5: Pressure drop (Laminar Flow)

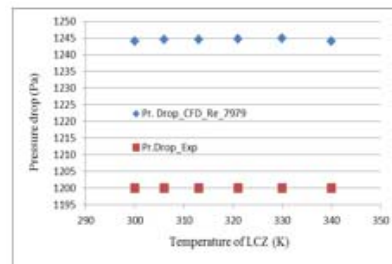


Figure 6: Pressure drop (Turbulent flow)

Overall trend in results are found to be similar between experiments and CFD as observed in Figure 7 and Figure 8. However, the difference of lower than 1 % comes due to unsteadiness and errors in experimental temperature measurements and numerical errors arising from CFD computations. This is evident from laminar & turbulent flows and also from the experimental values & CFD results. Thus for the remaining analysis, LCZ height of 200 mm alone is considered, this indicates only four cases were taken into consideration for analysis.

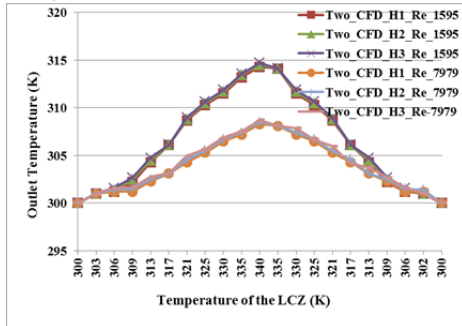


Figure 7: Outlet water temperature (CFD outputs)

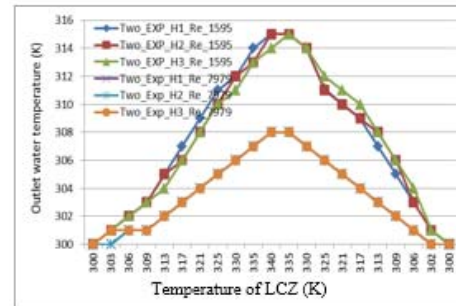


Figure 8: Outlet water temperature (Experimental)

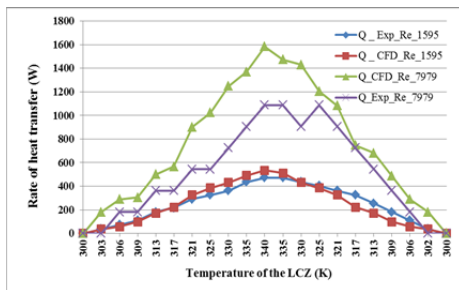


Figure 9: Rate of heat transfer

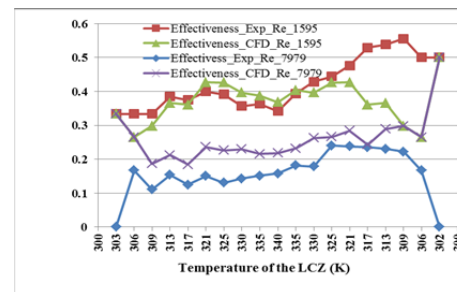


Figure 10: Effectiveness of heat exchanger

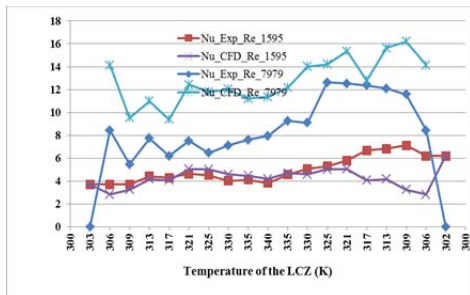


Figure 11: Nusselt Number

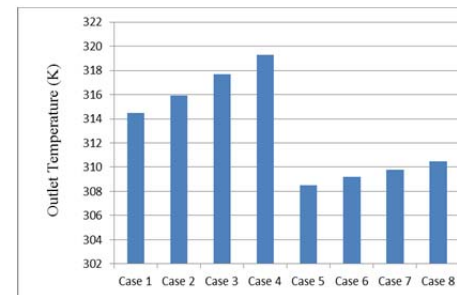


Figure 12: Variation of outlet water temperature for various swirl flow conditions

The rate of heat transfer from all the four cases of study is shown in Figure 9. It is observed the heat transfer is higher for turbulent flow than laminar flow, also the heat transfer is more when the temperature of the LCZ is higher at noon. The trend is same from computational and experimental results. This occurs due to higher pressure drop in turbulent flow. The heat transfer coefficient is related to Nusselt number ($Nu = 0.023 Re^{0.8} Pr^{0.33}$). Reynolds number relates the velocity which is obtained by pressure drop equation. ($\Delta p = fL v^2 / 2gD$). The effectiveness of heat exchanger is the ratio of actual rate of heat transfer to maximum rate of heat transfer which is represented in Figure 10. The maximum possible rate of heat transfer is determined between the LCZ temperature and the inlet water temperature. The effectiveness of heat exchanger is higher for laminar flow compared to turbulent flow. The trend of the curve is that the effectiveness increases as the temperature of LCZ increases this is because the period of exposure of SGSP is also more. From Figure 11, the values of Nusselt number are higher for turbulent condition and in all the cases, the value of Nusselt number is higher during noon, since the solar irradiation is more during this time and the heat exchange

process is also better. The novelty of the present work lies in the study of swirl at the heat exchanger inlet which influences the heat transfer from the LCZ solar pond. The results of purely axial component flow from CFD study are comparable with Alcaraz et al [1]. The important performance parameter for a SGSP is its outlet water temperature, since the remaining performance parameters like Nusselt number, rate of heat transfer and effectiveness are derived from outlet water temperature. Thus the variation of outlet water temperature for all the swirl flow cases (as discussed in table 4) considered under laminar and turbulent are shown in Fig. 12.

5. Conclusion

The following observations were obtained from the experimental and computational study carried out on the laboratory model SGSP. The computational model developed is providing results which are comparable with the experimental results. The variation of LCZ does not provide much variation in the outlet temperature. The Nusselt number for the turbulent flow is higher compared to laminar flow and hence the rate of heat transfer for the turbulent flow is greater. The increase in rate of heat transfer in turbulent flow is also due to higher pressure drop in turbulent flow. This is clearly visible from the pressure drop characteristics between the laminar and turbulent flows. Even though the rate of heat transfer is higher for the turbulent flow, the effectiveness of the heat exchanger is more for laminar flow. This indicates the temperature rise is higher for laminar flow but the mass flow rate is less as the velocity of flow is less. Also, as the velocity of flow is less in laminar flow, the residence time of the heat transfer fluid in the flow passage is higher and hence the higher degree of temperature rise. The performance parameter effectiveness is nothing but the second law efficiency of the SGSP. In the computational study, swirls were introduced in the flow field of the heat transfer fluid. This resulted with better mixing of the fluid leading to better rate of heat transfer. While comparing the laminar and turbulent flows, swirls in the flow field are more effective for laminar flow. This swirl in the flow has to be experimented in the near future in order to augment the rate of heat transfer in the SGSP. Due to the induction of swirl, the next phase of work includes the study of secondary flow at the pipe bend.

References

- Alcaraz A., Valderrama C., Cortina J.L., Akbarzadeh A., Farran A., 2016, Enhancing the efficiency of solar pond heat extraction by using both lateral and bottom heat exchangers, *Solar Energy*, 134, 82–94.
- Andreja Nemet., Jiří J. Klemeš, Moon, Zdravko Kravanja, 2017, Synthesis of Safer Heat Exchanger Networks, *Chemical Engineering Transactions*, 56, 1885-1890.
- Assad H.S., Hazim A.H., Alasdair N.C., 2016, New theoretical modelling of heat transfer in solar ponds, *Solar Energy*, 125, 207–218.
- Ayhan A., Ismail B., Mehmet K., Ibrahim D., 2014, Investigation of turbidity effect on exergetic performance of solar ponds, *Energy Conversion and Management*, 87, 351–358.
- Behrooz M.Z., Mehdi S., Mohammad N., 2016, Comparatively study between single-phase and two-phase modes of energy extraction in a salinity-gradient solar pond power plant, *Energy*, 111, 126-136.
- Ding L.C., Akbarzadeh A., Date A., 2016, Transient model to predict the performance of thermoelectric generators coupled with solar pond, *Energy*, 103, 271–289.
- Dipankar D., Tarun K.P., Santanu B., 2017, Helical baffle design in shell and tube type heat exchanger with CFD analysis, *International Journal of Heat and Technology*, 35(2), 378-383, DOI: 10.18280/ijht.350221
- Ganesh S., Aruugam S., 2016, Performance study of a laboratory model shallow solar pond with and without single transparent glass cover for solar thermal energy conversion applications, *Ecotoxicology and Environmental Safety*, 134(Pt 2), 462-466, DOI: 10.1016/j.ecoenv.2016.03.020.
- Huseyin K., Mehmet O., Korhan B., 2006, Experimental and numerical analysis of sodium-carbonate salt gradient solar pond performance under simulated solar radiation, *Applied Energy*, 83, 324-342.
- Ismail B., Mehmet K., 2015, The effect of sunny area ratios on the thermal performance of solar ponds, *Energy Conversion and Management*, 91, 323–332.
- Mohammad R.A., Hassan B.T., Ali K.N., Mohsen P., 2015, Experimental investigation of heat absorption of different solar pond shapes covered with glazing plastic, *Solar Energy*, 122, 569–578.
- Pesteei S.M., Nemat M., Saman P., Ashkan R., 2017, Numerical investigation on the effect of a modified corrugated double tube heat exchanger on heat transfer enhancement and exergy losses, *International Journal of Heat and Technology*, 35(2), 243-248, DOI: 10.18280/ijht.350202
- Pullela K.S., Ramakrishna K., Tunuguntla S., Lankapalli S.V.P., Viswanatha S.K., Vadapalli S., Dharma R.V., Veerapanen S.R.K.P., 2017, Fouling and its effect on the thermal performance of heat exchanger tubes, *International Journal of Heat and Technology*, 35(3), 509-519, DOI: 10.18280/ijht.350307
- Suraya H., Mohd K.A.,H., Sharifah R.W.A., Zainuddin A.M., 2017, An Industrial Case Study Application in Synthesising a Feasible Heat Exchanger Network, *Chemical Engineering Transactions*, 56, 775-780, DOI: 10.3303/CET1756130.